Immunology:

# T-cell Receptor (TCR)-Peptide Specificity Overrides Affinity-enhancing TCR-Major Histocompatibility Complex Interactions

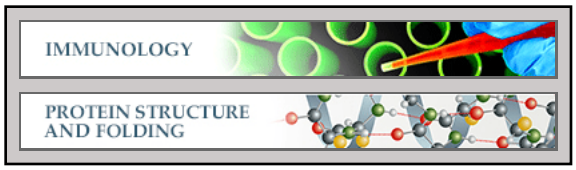


David K. Cole, Kim M. Miles, Florian Madura, Christopher J. Holland, Andrea J. A. Schauenburg, Andrew J. Godkin, Anna M. Bulek, Anna Fuller, Hephzibah J. E. Akpovwa, Phillip G. Pymm, Nathaniel Liddy, Malkit Sami, Yi Li, Pierre J. Rizkallah, Bent K. Jakobsen and Andrew K. Sewell

*J. Biol. Chem. 2014, 289:628-638.*
*doi: 10.1074/jbc.M113.522110 originally published online November 6, 2013*

---

THE JOURNAL OF BIOLOGICAL CHEMISTRY VOL. 289, NO. 2, pp. 628–638, January 10, 2014


# T-cell Receptor (TCR)-Peptide Specificity Overrides Affinity-enhancing TCR-Major Histocompatibility Complex Interactions*

Received for publication, September 27, 2013, and in revised form, October 22, 2013 Published, JBC Papers in Press, November 6, 2013, DOI 10.1074/jbc.M113.522110

**David K. Cole[‡1], Kim M. Miles[‡], Florian Madura[‡2], Christopher J. Holland[‡], Andrea J. A. Schauenburg[‡], Andrew J. Godkin[‡], Anna M. Bulek[‡], Anna Fuller[‡], Hephzibah J. E. Akpovwa[‡], Phillip G. Pymm[‡§], Nathaniel Liddy[¶], Malkit Sami[¶], Yi Li[¶], Pierre J. Rizkallah[‡], Bent K. Jakobsen[¶], and Andrew K. Sewell[‡3]**

*From [‡]Cardiff University School of Medicine, Heath Park, Cardiff CF14 4XN, the [§]Medical Research Council Human Immunology Unit, Weatherall Institute for Molecular Medicine, University of Oxford, Oxford 0X3 9DS, and [¶]Immunocore Ltd., 57C Milton Park, Abingdon OX14 4RX, United Kingdom*

**Background:** TCR recognition of bipartite ligands composed of self (MHC) and non-self (peptide) maintains T-cell specificity.
**Results:** Mutation of residues in the cognate peptide override TCR mutations that enhance MHC binding.
**Conclusion:** TCR-pMHC binding affinity requires specific TCR-peptide interactions.
**Significance:** Stabilization of TCR-pMHC engagement by TCR-peptide interactions maintains T-cell specificity and prevents recognition of self-pMHC in the periphery.

***αβ* T-cell receptors (TCRs) engage antigens using complementarity-determining region (CDR) loops that are either germ line-encoded (CDR1 and CDR2) or somatically rearranged (CDR3). TCR ligands compose a presentation platform (major histocompatibility complex (MHC)) and a variable antigenic component consisting of a short "foreign" peptide. The sequence of events when the TCR engages its peptide-MHC (pMHC) ligand remains unclear. Some studies suggest that the germ line elements of the TCR engage the MHC prior to peptide scanning, but this order of binding is difficult to reconcile with some TCR-pMHC structures. Here, we used TCRs that exhibited enhanced pMHC binding as a result of mutations in either CDR2 and/or CDR3 loops, that bound to the MHC or peptide, respectively, to dissect the roles of these loops in stabilizing TCR-pMHC interactions. Our data show that TCR-peptide interactions play a strongly dominant energetic role providing a binding mode that is both temporally and energetically complementary with a system requiring positive selection by self-pMHC in the thymus and rapid recognition of non-self-pMHC in the periphery.**

*αβ* T-cells protect against pathogens and cellular malignancies by recognizing short peptide fragments bound to major histocompatibility complex (pMHC)[4] molecules (1, 2). The rigors of T-cell immunity require that TCRs bind to self-pMHC during thymic selection but discriminate between self and non-self-pMHC thereafter by the rapid scanning of huge numbers of potential antigens on the target cell surface (3, 4). Here, we examine how TCR interactions with the variable peptide component of the antigen are balanced against contacts with the MHC to enable T-cells to activate if sensing danger, while remaining tolerant to self.

X-ray crystallographic studies have shown that the *αβ* TCR docks diagonally across the pMHC class I (pMHCI) peptide binding groove with the TCR *α* chain contacting the MHCI *α*2 helix and the TCR *β* chain contacting the MHCI *α*1 helix (5). A similar diagonal binding modality has been observed for TCR-pMHC class II interactions with the TCR *α* chain contacting the MHCII *β*1 helix and the TCR *β* chain contacting the MHCI *α*1 helix. This fixed polarity is conserved in all published TCR-pMHCI structures to date, although the binding angle and contacts between individual TCR-pMHCI complexes can vary substantially (5). TCR recognition of pMHC is mediated through the TCR complementarity-determining region (CDR) loops. Although not the case with all TCR-pMHC pairs (6), the current dogma proposes that the germ line-encoded TCR CDR2 loops contact mainly the conserved helical region of the MHC surface (TCR-MHC self-interaction); the somatically rearranged, hypervariable CDR3 loops contact mainly the antigenic peptide (TCR-peptide non-self interaction), and the CDR1 loops lie in between, contacting both the peptide and the MHC (5).

This binding conformation has led to the suggestion that TCRs contact MHC in a genetically conserved manner (7–10). Indeed, a study by Wu *et al.* (11) investigating the role of the TCR CDR loops during pMHC binding concluded that an initial transition state is formed between the TCR and the MHC surface enabling the TCR to scan the antigenic peptide (two-step binding) (12). This two-step binding model is considered to represent an important mechanism of allowing T-cells to sample a diverse array of pMHC antigens (3, 4, 13). In support

* This work was funded by Royal Society Grant RG080077, Wellcome Trust Program Grant WT086716MA, and Biotechnology and Biological Sciences Research Council Grant BB/H001085/1.
⌘ *Author's Choice*—Final version full access.
*The atomic coordinates and structure factors (code 4MNQ) have been deposited in the Protein Data Bank (http://wwpdb.org/).*
[1] Wellcome Trust Research Career Development Fellow supported by Grant WT095767. To whom correspondence may be addressed. Tel.: 442920687006; E-mail: coledk@cf.ac.uk.
[2] Supported by a Tenovus Ph.D. studentship.
[3] To whom correspondence may be addressed. Tel.: 442920687055; E-mail: sewellak@cf.ac.uk.
[4] The abbreviations used are: pMHC, peptide-major histocompatibility complex; SPR, surface plasmon resonance; TCR, T-cell receptor; CDR loop, complementarity-determining region loop; PDB, Protein Data Bank; MHCI, pMHC class I.

of this notion, combined studies have suggested the existence of so-called "interaction codons" that enable the TCR to contact the MHC surface in a conserved manner (7–10). Furthermore, structural comparison of different TCRs with genetically identical CDR2$\beta$ loops, in complex with the same pMHC, lends support to the idea that some TCRs may use genetically fixed pairwise interactions to bind to the MHC surface (9, 14). In combination, these data predict that interactions between the TCR and MHC stabilize the initial "encounter complex." However, there is also a body of evidence that contradicts this model of TCR binding (15–21). Thus, there is still much controversy over this central question concerning the nature of T-cell antigen recognition.

The binding affinity of natural TCR-pMHC interactions ($K_D$~ 0.1–500 $\mu$M) (22, 23) is near the limits of detection using current biophysical techniques. This restricts the scope for investigating TCR-pMHC interactions by mutating important contacts, because altering this weak interaction often results in the loss of any detectable binding using surface plasmon resonance (SPR). To examine the roles of the TCR CDR loops when binding to pMHC, we designed a range of enhanced affinity soluble TCRs with mutations in either their CDR2 and/or CDR3 loops. These unique enhanced affinity reagents enabled investigation of the effects of altering specific interactions between the TCR and MHC or TCR and peptide to examine how individual components of the interface between the TCR and pMHCI contribute to T-cell antigen recognition. These data shed new light on how T-cells might be selected in the thymus to maintain tolerance to self, the mechanism of T-cell cross-reactivity, and the nature of T-cell antigen recognition.

## EXPERIMENTAL PROCEDURES

*Generation of Expression Plasmids*—A number of constructs were prepared that contained wild type and high affinity TCRs to the HLA A*0201-restricted antigens, Melan-A/MART-1(26–35) ELAGIGILTV (24) and hTERT(540–548) ILAKFLHWL (25). The HLA A*0201-ELAGIGILTV- and HLA A*0201-ILAKFLHWL-specific wild type TCRs (MEL5 and ILA1 TCRs, respectively), the high affinity TCR $\alpha$ and $\beta$ chains, HLA A*0201 heavy chain, and $\beta$2m were generated by PCR mutagenesis (Stratagene) and PCR cloning. All sequences were confirmed by automated DNA sequencing (Lark Technologies). The high affinity HLA A*0201-ELAGIGILTV and HLA A*0201-ILAKFLHWL TCRs were produced using a phage display library as reported previously (26). All of the TCR sequences were constructed implementing a disulfide-linked construct to produce the soluble domains (variable and constant) for both the $\alpha$ (residues 1–207) and $\beta$ chains (residues 1–247) (27, 28). The HLA A2 heavy chain (residues 1–248) ($\alpha$1, $\alpha$2, and $\alpha$3 domains), tagged with a biotinylation sequence, and $\beta$2m (residues 1–100) were also cloned and used to make the pMHCI complexes. The TCR $\alpha$ and $\beta$ chains, the HLA A2 $\alpha$ chain and $\beta$2m sequences were inserted into separate pGMT7 expression plasmids under the control of the T7 promoter (27).

*Protein Expression, Refolding, and Purification*—Competent Rosetta DE3 *Escherichia coli* cells were used to produce the TCR $\alpha$ and $\beta$ chains, HLA A*0201 heavy chain and $\beta$2m in the form of inclusion bodies using 0.5 mM isopropyl 1-thio-$\beta$-D-galactopyranoside to induce expression as described previously (27, 29, 30).

*pMHCI Biotinylation*—Biotinylated pMHCI was prepared as described previously (31).

*SPR Equilibrium Analysis*—The binding analysis was performed using a BIAcore T100™ equipped with a CM5 sensor chip as reported previously (32).

*SPR Kinetic Analysis*—Experiments were carried out to determine the $K_{on}$ and $K_{off}$ values for the TCRs at 25 °C as reported previously (33). Briefly, for all kinetic experiments, ~300 response units of pMHC were coupled to the CM5 sensor chip surface. The TCR was then injected at concentrations ranging from 10 times above and 10 times below the known $K_D$ value of the interaction at 45 $\mu$l/min. The $K_{on}$ and $K_{off}$ values were calculated assuming 1:1 Langmuir binding ($AB = B{\cdot}AB_{max}/(K_D + B)$), and the data were analyzed using a global fit algorithm (BIAevaluation™ 3.1).

*SPR Kinetic Titration Analysis*—To stringently examine the binding of the TCRs at a greater range of concentrations, we used a new method for analyzing the kinetic parameters of high affinity interactions with long off rates (34). Each TCR was analyzed at five concentrations that represented the greatest range we could accurately achieve around the $K_D$ value of each interaction. During the analysis, ~300 response units of pMHC were immobilized onto the CM5 sensor chip surface. Each concentration of TCR was injected at a high flow rate of 45 $\mu$l/min for a 240-s association period and a 120-s dissociation period. The final and highest concentration had a longer dissociation period of 600 s. A fast flow rate and a low amount of immobilized pMHC were used to limit association and dissociation mass transfer limitations as recommended by the experts at BIAcore™. The $K_{on}$ and $K_{off}$ values were calculated assuming 1:1 Langmuir binding ($AB = B{\cdot}AB_{max}/(K_D + B)$), and the data were analyzed using the kinetic titration analysis algorithm (BIAevaluation™ Version 3.1) (35).

*Crystallization and X-ray Data Collection*—$\alpha$1$\beta$1-A2-ILA crystals were grown in 20 mM Tris, pH 7.5, 20% PEG 4000, and 10 mM NaCl. All crystals were soaked in 30% ethylene glycol before cryo-cooling. Data were collected at 100 K at the Diamond Light Source, UK. Reflection intensities were estimated with the XIA2 package (36), and the data were scaled, reduced, and analyzed with SCALA and the CCP4 package (37). Structures were solved with molecular replacement using PHASER (38). Sequences were adjusted with COOT (39), and the models were refined with REFMAC5. Graphical representations were prepared with PyMOL (40). The reflection data and final model coordinates were deposited with the PDB database ($\alpha$1$\beta$1-A2-ILA, PDB 4MNQ).

## RESULTS

*Design of a Panel of High Affinity TCRs Specific for Two Different HLA A*0201-restricted Peptides*—Investigating the individual roles of the TCR CDR loops when binding to pMHC has been difficult because the weak binding affinities of natural TCR-pMHC interactions (0.1–500 $\mu$M) (22, 23) are close to the limits of detection by SPR. To overcome this problem, we designed a range of soluble TCRs with up to 18,500-fold enhancement in affinity for cognate antigen using CDR loop

mutations selected by phage display (Table 1) (26). We first measured the binding affinity and kinetics of wild type and enhanced affinity TCRs specific for either the HLA A*0201-restricted peptide antigens, Melan-A/MART-1(26–35) (ELAGIGILTV), or hTERT(540–548) (ILAKFLHWL). The HLA A*0201-ELAGIGILTV-specific TCRs with mutated CDR2 or CDR2 and CDR3 loops bound with considerably stronger affinities ($K_D$s between 12 and 897 times greater) than the parent wild type TCR (MEL5) (Fig. 1 and Table 2). The HLA A*0201-ILAKFLHWL specific TCRs with mutated CDR2 loops bound to cognate antigen with a substantially stronger affinity ($K_D$ values between 1423 and 4066 times greater) compared with the parent wild type TCR (ILA1) (Fig. 2 and Table 3). Similarly, when the mutated CDR2 and CDR3 loop mutations were combined, we observed a further increase in binding affinity ($K_D$ values up to 18,500 times greater than ILA1 TCR), indicating that the mutations could be used cooperatively (Fig. 3 and Table 3). In agreement with our previous findings (26, 34, 41–44), enhanced TCR affinity was due to small increases in the on-rate, and vastly extended off-rates (Tables 2 and 3, Figs. 1–3). The stronger affinities of the high affinity TCRs enabled the modulation of individual components of the TCR-peptide interaction through peptide mutations while maintaining enough residual binding to detect using SPR in later experiments.

**TABLE 1**
**Sequence comparison of high affinity TCRs**

| TCR | Mutation | CDR2β$_{56-60}$ | CDR3β$_{104-119}$ |
|---|---|---|---|
| **MEL5** | wildtype | SVGIG | CAWSETGLGTGELFFG |
| MEL5β1 | CDR2 | **YGPF**G | |
| MEL5β2 | CDR2 | **WGPF**G | |
| MEL5β3 | CDR2 | **FGPY**G | |
| MEL5β4 | CDR2 | **YGPY**G | |
| MEL5β5 | CDR2&3 | **YGPF**G | CAWSETGLG**M**G**GWQ**FG |
| MEL5β6 | CDR2&3 | **YGPF**G | CAWSETGL**NL**G**GW**FFG |
| MEL5β7 | CDR2&3 | **WGPF**G | CAWSETGLG**M**G**GWQ**FG |
| MEL5β8 | CDR2&3 | **WGPF**G | CAWSETGL**NL**G**GW**FFG |
| TCR | Mutation | CDR2β$_{49-54}$ | CDR3α$_{104-119}$ |
| **ILA1** | wildtype | SVGAGI | CAVDSATSGTYKYIFG |
| ILA1β1 | CDR2 | S**IHPEY** | |
| ILA1β2 | CDR2 | S**IWEFE** | |
| ILA1α1 | CDR3 | SVGAGI | CAVDSAT**ALP**Y**G**YIFG |
| ILA1α1β1 | CDR2&3 | S**IHPEY** | CAVDSAT**ALP**Y**G**YIFG |
| ILA1α1β2 | CDR2&3 | S**IWEFE** | CAVDSAT**ALP**Y**G**YIFG |

*High Affinity CDR2 Loop Mutated TCRs Do Not Bind to "Null" Peptides*—Our recent structure of a high affinity variant of the MEL5 TCR (34) demonstrated that the mutated CDR2α region of the high affinity MEL5-derived TCRs used in this study was in an identical position to the wild type MEL5 TCR (24), distal from the peptide (Fig. 4, *A* and *B*). Thus, we concluded that mutations at residues in the peptide were very unlikely to directly affect the high affinity interactions between the MEL5 derived high affinity TCRs and the MHC surface. We reasoned that, because the general dogma of TCR engagement postulates that TCR-MHC interactions bind before TCR-peptide sampling, the high affinity interaction between the MEL5-derived TCRs and the MHC surface should retain some measurable ability to bind to the surface of HLA A2 irrespectively of the bound peptide, because the interaction between the TCR and the peptide should only account for a small proportion of the overall binding energy (δG). To investigate the role of pep-

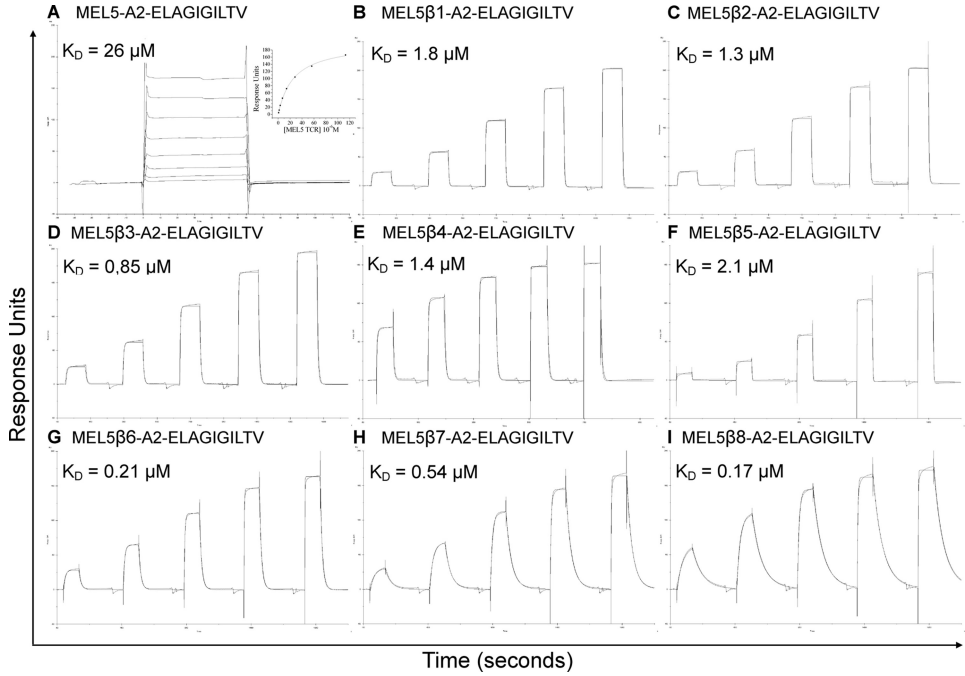


FIGURE 1. **Affinity and kinetic analysis of wild type and high affinity MEL5-derived TCRs.** *A–I,* these data were produced using a BIAcore T100™ and were then analyzed using equilibrium analysis, kinetic global fit analysis, and kinetic titration analysis. The raw data and the fits are shown in each panel. These data illustrate the improved binding capabilities of the high affinity mutant HLA A2-ELAGIGILTV-specific TCRs compared with the MEL5 TCR. None of the HLA A2-ELAGIGILTV-specific TCRs bound to the HLA A2-ELAGIGILTV with alanine or glycine substitutions.

**TABLE 2**

**Kinetic and affinity analysis of high affinity HLA-A*0201-ELAGIGILTV-specific TCR binding to alanine- and glycine-substituted peptides**

| TCR | Mutation | $K_{on}M^{-1}s^{-1}$ | $K_{off}s^{-1}$ | $K_D$ | Half-life Min | ΔG kcal/mol$^{-1}$ |
|---|---|---|---|---|---|---|
| | | HLA A*0201-ELAGIGILTV | | | | |
| **MEL5** | wildtype | N/M | N/M | 26±2.1 μM | N/M | -5.83 |
| MEL5β1 | CDR2 | $1.4x10^5$ | $2.6x10^{-1}$ | 1.8±0.4 μM | 0.04 | -7.31 |
| MEL5β2 | CDR2 | $2 x10^5$ | $2.6x10^{-1}$ | 1.3±0.3 μM | 0.04 | -7.49 |
| MEL5β3 | CDR2 | $1.8x10^5$ | $1.6x10^{-1}$ | 0.85±0.1 μM | 0.07 | -7.72 |
| MEL5β4 | CDR2 | $1.6x10^5$ | $2.3x10^{-1}$ | 1.4±0.2 μM | 0.05 | -7.45 |
| MEL5β5 | CDR2&3 | $2.5x10^5$ | $5.2x10^{-1}$ | 2.1±0.5 μM | 0.02 | -7.22 |
| MEL5β6 | CDR2&3 | $2.9x10^5$ | $6.1x10^{-2}$ | 0.21±0.33 μM | 0.19 | -8.49 |
| MEL5β7 | CDR2&3 | $4.6x10^4$ | $2.5x10^{-2}$ | 0.54±0.1 μM | 0.46 | -7.97 |
| MEL5β8 | CDR2&3 | $8x10^4$ | $1.4x10^{-2}$ | 0.17±0.1 μM | 0.82 | -8.61 |
| | | HLA A*0201-ALAAAAAAV | | | | |
| | | HLA A*0201-GLGGGGGGV | | | | |
| | | HLA A*0201-**A**LAGIGILTV | | | | |
| | | HLA A*0201-ELA**A**IGILTV | | | | |
| | | HLA A*0201-ELAG**A**GILTV | | | | |
| | | HLA A*0201-ELAGI**A**ILTV | | | | |
| | | HLA A*0201-ELAGIG**A**LTV | | | | |
| | | HLA A*0201-ELAGIGI**A**TV | | | | |
| | | HLA A*0201-ELAGIGIL**A**V | | | | |
| **MEL5** | wildtype | NO BINDING | | | | |
| MEL5β1 | CDR2 | NO BINDING | | | | |
| MEL5β2 | CDR2 | NO BINDING | | | | |
| MEL5β3 | CDR2 | NO BINDING | | | | |
| MEL5β4 | CDR2 | NO BINDING | | | | |
| MEL5β5 | CDR2&3 | NO BINDING | | | | |
| MEL5β6 | CDR2&3 | NO BINDING | | | | |
| MEL5β7 | CDR2&3 | NO BINDING | | | | |
| MEL5β8 | CDR2&3 | NO BINDING | | | | |

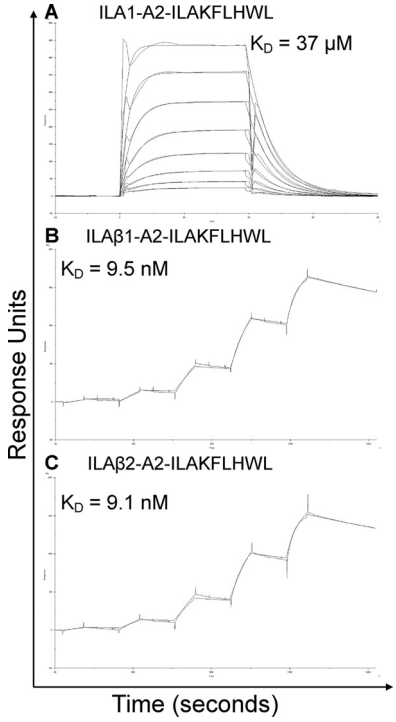


FIGURE 2. **Affinity and kinetic analysis of wild type and high affinity ILA1-derived TCRs.** *A–C,* these data were produced using a BIAcore T100™ and were then analyzed using equilibrium analysis, kinetic global fit analysis, and kinetic titration analysis. The raw data and the fits are shown in each panel. These data show that the ILA1$\beta$1 and ILA1$\beta$2 TCRs bound to HLA A*0201-ILAKFLHWL with ~4000 times greater affinity than the wild type ILA1 TCR.

tide modifications on TCR-pMHC docking, we manufactured two null HLA A*0201-nonamer peptide complexes where nonprimary MHC anchors were substituted with either glycine or alanine. However, we were unable to detect binding of any of the HLA A*0201-ELAGIGILTV- or HLA A*0201-ILAKFLHWL-specific high affinity TCRs tested against the HLA

**TABLE 3**

**Kinetic and affinity analysis of high affinity HLA-A*0201-ILAKFLHWL-specific TCRs binding to alanine- and glycine-substituted peptides**

| TCR | Mutation | $K_{on}M^{-1}s^{-1}$ | $K_{off}s^{-1}$ | $K_D$ M | Half-life Min | ΔG kcal/mol$^{-1}$ | *ΔΔG kcal/mol$^{-1}$ |
|---|---|---|---|---|---|---|---|
| | | HLA A*0201-ILAKFLHWL | | | | | |
| **ILA1** | wildtype | $3.5x10^5$ | $1.3x10^{-1}$ | 37±5 μM | 0.09 | -5.64 | N/A |
| ILA1β1 | CDR2 | $3.0x10^4$ | $2.9x10^{-4}$ | 9.5±1.1 nM | 39.66 | -10.20 | N/A |
| ILA1β2 | CDR2 | $3.1x10^4$ | $2.8x10^{-4}$ | 9.1±1.1 nM | 41.07 | -10.23 | N/A |
| ILA1α1 | CDR3 | $2.4x10^4$ | $6.3x10^{-4}$ | 26±4 nM | 18.25 | -9.65 | N/A |
| ILA1α1β1 | CDR2&3 | $8.0x10^4$ | $1.6x10^{-4}$ | 2.0±1 nM | 71.88 | -11.06 | N/A |
| ILA1α1β2 | CDR2&3 | $1.4x10^5$ | $4.3x10^{-4}$ | 3.1±1.2 nM | 26.74 | -10.82 | N/A |
| | | HLA A*0201-ALAAAAAAV | | | | | |
| | | HLA A*0201-GLGGGGGGV | | | | | |
| **ILA1** | wildtype | NO BINDING | | | | N/A | |
| ILA1β1 | CDR2 | NO BINDING | | | | N/A | |
| ILA1β2 | CDR2 | NO BINDING | | | | N/A | |
| ILA1α1 | CDR3 | NO BINDING | | | | N/A | |
| ILA1α1β1 | CDR2&3 | NO BINDING | | | | N/A | |
| ILA1α1β2 | CDR2&3 | NO BINDING | | | | N/A | |
| | | HLA A*0201-ILA**A**FLHWL | | | | | |
| **ILA1** | wildtype | NO BINDING | | | | N/A | |
| ILA1β1 | CDR2 | $8.2x10^3$ | $7.5x10^{-3}$ | 0.92±0.1 μM | 1.53 | -7.68 | 2.53 |
| ILA1β2 | CDR2 | NO BINDING | | | | N/A | |
| ILA1α1 | CDR3 | $3.2x10^3$ | $8.5x10^{-3}$ | 2.6±0.2 μM | 1.35 | -7.10 | 2.54 |
| ILA1α1β1 | CDR2&3 | $3.8x10^3$ | $3.1x10^{-2}$ | 8.3±1 μM | 0.37 | -6.46 | 4.60 |
| ILA1α1β2 | CDR2&3 | $3.4x10^4$ | $2.8x10^{-1}$ | 8.4±1.1 μM | 0.04 | -6.46 | 4.37 |
| | | HLA A*0201-ILAKF**A**HWL | | | | | |
| **ILA1** | wildtype | NO BINDING | | | | N/A | |
| ILA1β1 | CDR2 | $4.4x10^3$ | $4.9x10^{-2}$ | 11±1 μM | 0.23 | -6.31 | 3.90 |
| ILA1β2 | CDR2 | $3.9x10^5$ | $7.3x10^{-2}$ | 19±2.2 μM | 0.16 | -6.01 | 4.22 |
| ILA1α1 | CDR3 | $1.0x10^4$ | $5.4x10^{-2}$ | 5.3±0.3 μM | 0.21 | -6.71 | 2.94 |
| ILA1α1β1 | CDR2&3 | $6.3x10^3$ | $1.4x10^{-2}$ | 2.2±0.1 μM | 0.82 | -7.20 | 3.87 |
| ILA1α1β2 | CDR2&3 | $1.5x10^4$ | $4.9x10^{-2}$ | 3.3±0.3 μM | 0.23 | -6.97 | 3.85 |

* $\Delta\Delta G^0 = \Delta G^0$ of each TCR binding to HLA A2-ILAKFLHWL alanine variants minus $\Delta G^0$ of TCR to HLA A2-ILAKFLHWL.

A*0201-GLGGGGGGV or HLA A*0201-ALAAAAAAV null antigens (Tables 2 and 3). These observations are remarkable when considering that, for example, the CDR2 loop modified ILA1$\beta$2 TCR bound to HLA A*0201-ILAKFLHWL with an affinity >4000 times greater than the wild type ILA1 TCR (Table 3 and Fig. 2). These data support the notion that specific interactions between the TCR and peptide are required to allow the TCR to effectively engage MHC and demonstrate that changes to the antigenic peptide override mutations in the TCR that enhance contacts with the MHC molecule.

*CDR2-mutated High Affinity HLA A*0201-ELAGIGILTV-specific TCRs Are Extraordinarily Sensitive to Peptide Substitutions*—To investigate the role of more conservative peptide modifications on TCR binding affinity, we introduced single alanine substitutions into the HLA A*0201-ELAGIGILTV (MART-1/Melan A-derived) peptide antigen. We substituted residues in the peptide that were very unlikely to directly affect the high affinity regions of the MEL5-derived high affinity TCRs and the MHC surface, according to our structural evidence (Fig. 4, *A* and *B*) (24, 34). This enabled the determination of the effect of altering TCR-peptide contacts on TCR-MHC binding. Neither the MEL5 TCR nor any of the high affinity TCRs retained the ability to bind to HLA A*0201-ELA**A**IGILTV, HLA A*0201-ELAGI-**A**ILTV, HLA A*0201-ELAGIG**A**LTV, or HLA A*0201-ELA-GIGIL**A**V (Table 2). This observation that single alanine substitutions in the native peptide can completely abrogate binding of all of the high affinity HLA A*0201-ELAGIGILTV-specific TCRs reaffirms the notion that specific interactions between the TCR and peptide are required in order for optimal docking with the MHC surface to occur, and this is consistent with our previous findings using this system (34).

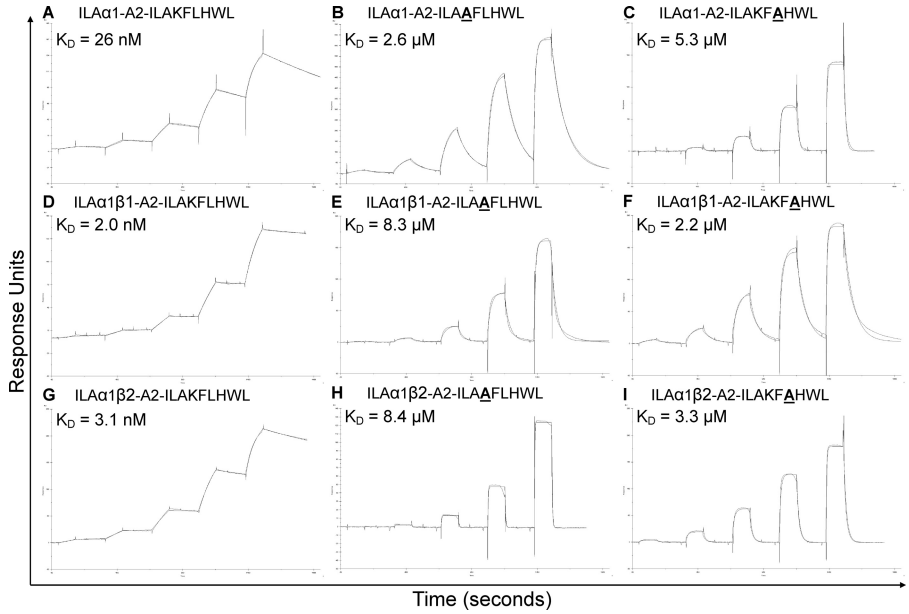


FIGURE 3. **Effect of alanine peptide substitutions on high affinity ILA1-derived TCR binding.** Binding affinity and kinetic analysis of the HLA A*0201-ILAKFLHWL-specific high affinity ILA1$\alpha$1, ILA1$\alpha$1$\beta$1, and ILA1$\alpha$1$\beta$2 TCRs to HLA A2-ILAKFLHWL, HLA A2-ILA**A**FLHWL, and HLA A2-ILAKF**A**HWL (*A–I*). These data were produced using a BIAcore T100$^{TM}$ and were then analyzed using equilibrium analysis, kinetic global fit analysis, and kinetic titration analysis. The raw data and the fits are shown in each panel. These data show the effect of the HLA A2-ILA**A**FLHWL and HLA A2-ILAK**A**LHWL peptide modifications on the binding of the high affinity TCRs compared with HLA A2-ILAKFLHWL. These support the notion that TCR-peptide interactions govern TCR-pMHC binding because, although the ILA1$\alpha$1$\beta$1 TCR with a mutated CDR2 loop did not contact the peptide, the difference in binding between the ILA1$\alpha$1 TCR and the ILA1$\alpha$1$\beta$1 TCR to HLA A2-ILA**A**FLHWL and HLA A2-ILAK**A**LHWL compared with HLA A2-ILAKFLHWL is disproportionately different.

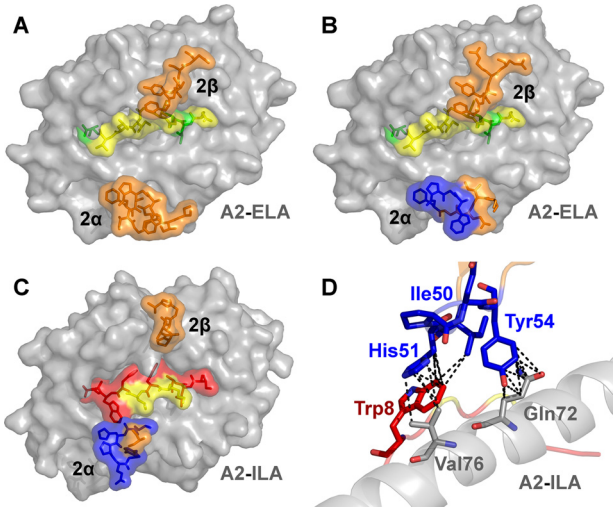


FIGURE 4. **Peptide modifications do not directly impinge on the binding of mutated high affinity TCR residues.** The complex structures of high affinity MEL5- and ILA1-derived TCRs show that peptide modifications do not directly impinge on the binding of mutated high affinity TCR residues. *A,* wild type MEL5-A2-ELA (PDB code 3HG1 (24)) complex structure showing the MHC in *gray surface*, the mutated peptide residues in *yellow stick* and *surface* (nonmutated residues in *green*), and the positions of the TCR CDR2 loops in *orange sticks* and *surface*. *B,* high affinity $\alpha$24$\beta$17-A2-ELA (PDB code 4JFF (34)) complex structure ($\alpha$24$\beta$17 is a high affinity version of the MEL5 TCR) showing the MHC in *gray surface*, the mutated peptide residues in *yellow stick* and *surface* (nonmutated residues in *green*), and the positions of the TCR CDR2 loops in *orange sticks* and *surface*. In this structure, the high affinity mutations in the TCR CDR2$\alpha$ loop are colored *blue* and are distal from the peptide. *C,* high affinity $\alpha$1$\beta$1-A2-ILA (PDB code 4MNQ) complex structure ($\alpha$1$\beta$1 is a high affinity version of the ILA1 TCR) showing the MHC in *gray surface*, the mutated peptide residues in *yellow stick* and *surface* (nonmutated residues in *red*), and the positions of the TCR CDR2 loops in *orange sticks* and *surface*. *D,* specific contacts between the high affinity mutated residues in the $\alpha$1$\beta$1 TCR CDR2$\alpha$ loop (*blue sticks*), the MHC (*gray sticks*), and the peptide (*red*). The peptide residues that were mutated to alanine (*yellow*) were not directly contacted by the high affinity mutated residues in the $\alpha$1$\beta$1 TCR CDR2$\alpha$ loop. Overall, these structures demonstrate that TCR residues that have been mutated in the CDR2 loops of high affinity TCRs do not directly contact residues that were mutated to alanine in the peptide.

*Affinity-enhanced CDR2α Loops of the ILA1-derived TCRs Do Not Contact Alanine-substituted Peptide Residues*—Previous structural comparisons of wild type and high affinity TCRs (34, 41–43) show that these molecules adopt a near identical binding mode (Fig. 5). To confirm that alanine substitutions of these peptide residues would not directly impinge on the mutated residues in the high affinity CDR2$\alpha$ loops of the ILA1-derived TCRs, we solved the structure of the ILA1$\alpha$1$\beta$1 TCR in complex with HLA A*0201-ILAKFLHWL. The complex was solved to a resolution of 2.4 Å in space group C121. The resolution was sufficiently high to show that the interface between the two molecules was well ordered and contained well defined electron density. The crystallographic $R/R_{free}$ factors were 20.1 and 24.6%, within the accepted limits shown in the theoretically expected distribution (Table 4) (45). The structure demonstrated that the mutated CDR2$\alpha$ region of the high affinity $\alpha$1$\beta$1 TCR could not directly contact the mutated residues in the peptide (Fig. 4, *C* and *D*, and Table 5).

*HLA A*0201-ILAKFLHWL Peptide Substitutions Disproportionately Affect the Binding of High Affinity CDR2 Loop Mutated TCRs*—We then measured the binding of the HLA A*0201-ILAKFLHWL-specific wild type ILA1 TCR and high affinity derivative TCRs to HLA A*0201-ILA**A**FLHWL and HLA A*0201-ILAKF**A**HWL (Table 3 and Fig. 3). The ILA1$\alpha$1 high affinity TCR bound to HLA A*0201-ILA**A**FLHWL and HLA A*0201-ILAKF**A**HWL with 100 and 200 times weaker affinity, respectively, than to HLA A*0201-ILAKFLHWL. This difference corresponded to a $\Delta\Delta G$ value (difference in binding energy, $\Delta G$, between the ILA1$\alpha$1 high affinity TCR interacting with HLA A*0201-ILAKFLHWL *versus* HLA A*0201-ILA**A**FLHWL and HLA A*0201-ILAKF***A***HWL) of 2.54 and 2.94 kcal/mol$^{-1}$, respectively. We then repeated this analysis using the

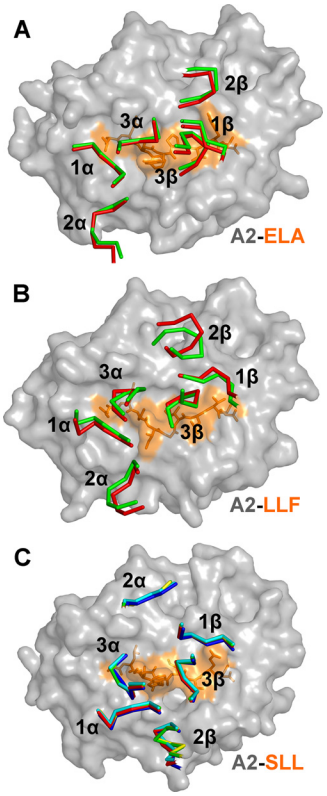


FIGURE 5. **Conformation of TCR CDR loops remains very similar between modified high affinity TCRs and their wild type progenitors.** Comparison of the CDR loop positions of previously published high affinity and wild type TCRs. *A,* wild type MEL5-A2-ELA complex (24) (CDR loops in *orange ribbon*) and the high affinity α24β17-A2-ELA complex (34) (CDR loops in *green ribbon*). *B,* wild type A6-A2-LLF complex (27) (CDR loops in *orange ribbon*) and the high affinity c134-A2-LLF complex (41) (CDR loops in *green ribbon*). *C,* wild type 1G4-A2-SLL complex (64) (CDR loops in *orange ribbon*) and the high affinity c58c62-A2-SLL (CDR loops in *green ribbon*), c49c50-A2-SLL (CDR loops in *blue ribbon*), c549c61-A2-SLL (CDR loops in *yellow ribbon*), and c5c1-A2-SLL (CDR loops in *cyan ribbon*) complexes (42, 43). In all cases, the relative positions of the CDR loops over the pMHC for the wild type TCRs and their high affinity TCR derivative are virtually identical.

**TABLE 4**
**Data collection and refinement statistics for α1β1-A2-ILA complex structure**
One crystal was used for solving the structure. Values in parentheses are for the highest resolution shell.

| | α1β1-A2-ILA |
|---|---|
| PDB code | 4MNQ |
| **Data collection** | |
| Space group | $P3_221$ |
| Cell dimensions | |
| *a*, *b*, *c* | 97.14, 97.14, 123.08 Å |
| α, β, γ | 90, 90, 120° |
| Resolution (Å) | 49.7 to 2.4 Å (10.7 to 2.4 Å) |
| $R_{merge}$ | 19.2% |
| $I/\sigma I$ | 16.6 |
| Completeness | 100% |
| Redundancy | 10.9 |
| **Refinement** | |
| Resolution | 2.4 Å |
| No. of reflections | 25,403 |
| $R_{work}/R_{free}$ | 20.1/24.6 |
| No. of atoms | 3694 |
| Protein | 3492 |
| Ligand/ion | 41 |
| Water | 161 |
| *B*-factors | 44.63 |
| Protein | 44.60 |
| Ligand/ion | 60.79 |
| Water | 41.10 |
| Root mean square deviations | |
| Bond lengths | 0.022 Å |
| Bond angles | 1.206° |

ILA1α1β1 and ILA1α1β2 TCRs. These TCRs contained modified CDR2 loops but identical CDR3 loops to the ILA1α1 TCR. According to the assumption that TCR-MHC interactions precede TCR-peptide interactions, we reasoned that each of these TCRs should retain their individual TCR-MHC contacts because only the TCR-peptide interaction should be directly affected (as in Fig. 6*A*). Therefore, the difference in binding affinity observed for the ILA1α1 TCR between HLA A*0201-ILAKFLHWL compared with HLA A*0201-ILA**A**FLHWL and HLA A*0201-ILAKF**A**HWL (100 and 200 times weaker affinity, respectively) should be similar to the ILA1α1β1 and ILA1α1β2 TCRs. However, the ILA1α1β1 TCR bound to the HLA A*0201-ILA**A**FLHWL and HLA A*0201-ILAKF**A**HWL with 4150 and 1100 times weaker affinity ($\Delta\Delta G$ value of 4.6 and 3.87 kcal/mol$^{-1}$), respectively (Table 3 and Figs. 3 and 6*B*). The ILA1α1β2 TCR bound to HLA A*0201-ILA**A**FLHWL and HLA A*0201-ILAKF**A**HWL with 2710 and 1065 times weaker affinity ($\Delta\Delta G$ value of 4.37 and 3.85 kcal/mol$^{-1}$), respectively (Table 3 and Fig. 3). These data demonstrate that TCR interactions with the peptide and MHC are strongly coupled and that modifying the TCR-peptide interaction has a disproportionately strong detrimental energetic effect on TCR-MHC binding.

*Effect of Peptide Substitutions on the Binding Kinetics of High Affinity CDR2 Loop Mutated TCRs*—Kinetic binding analyses were carried out at 25 °C to measure the on-rate ($K_{on}$) and off-rate ($K_{off}$) for each TCR-pMHCI interaction (Figs. 1–3 and Tables 2 and 3). These analyses were important to reveal the kinetic basis for the effect of altering the TCR-peptide interactions by modifying the antigenic peptide. Interestingly, although alanine mutations within the central peptide residues reduced the binding affinity of all of the high affinity TCRs tested to a different extent (97–4150-fold reduction in binding affinity), the on-rate was not substantially affected (average decrease of 10 times) (Tables 2 and 3). Conversely, the stability of the TCR-pMHC complex was affected by a greater extent, as evident by the faster off-rate observed (average increase of 200 times) (Tables 2 and 3). Therefore, a faster off-rate was the major kinetic determinant governing the decrease in binding affinity between the high affinity CDR loop mutated TCRs and the alanine-substituted peptide ligands. These data suggest that in order for the TCR to form a stable long lived interaction with cognate pMHC, the TCR must be able to bind to the peptide to allow optimal MHC docking. Thus, in the systems we have studied, successful TCR-peptide sampling must precede (or occur at the same time as) the stabilizing interaction between the TCR and the MHC surface.

## DISCUSSION

Antigen recognition by the TCR usually involves contacts with both self (MHC) and non-self (the antigenic peptide) (5, 16). To avoid autoreactivity, the self-interaction between the TCR and MHC must not be sufficient to activate peripheral T-cells independently of the non-self TCR-peptide interaction. The current database of TCR-pMHC complex structures

**TABLE 5**
**$\alpha 1\beta 1$-A2-ILA contacts (residues mutated from wild type shown in red)**

| TCR | Gene Usage | TCR | Peptide | MHC | vdW (≤4 Å) | H-bonds (≤3.4 Å) |
|---|---|---|---|---|---|---|
| CDR1α | *TRAV22* | $Asp27^{O\delta 2}$ | | $Thr163^{O\gamma 1}$ | 4 | 1 |
| | *TRAV22* | Asp27 | | Glu166 | 1 | |
| | *TRAV22* | Ser28 | | Ala158 | 1 | |
| | *TRAV22* | Val29 | | Gln155 | 5 | |
| | *TRAV22* | Val29 | Lys4 | | 2 | |
| | *TRAV22* | $Asn30^{O\delta 1}$ | | $Gln155^{O\varepsilon 1}$ | 3 | 1 |
| CDR2α | *TRAV22* | Tyr48 | | Glu155 | 1 | |
| | *TRAV22* | Pro50 | | Glu154 | 1 | |
| | *TRAV22* | Ser51 | | Glu154 | 3 | |
| | *TRAV22* | Ser51 | | Arg157 | 1 | |
| | *TRAV22* | $Gln55^{N\varepsilon 2}$ | | $Glu154^{O\varepsilon 2}$ | 1 | 1 |
| FWα | *TRAV22* | Thr66 | | Glu166 | 1 | |
| | *TRAV22* | $Arg68^{NH2}$ | | $Glu166^{O\varepsilon 2}$ | 2 | 1 salt bridge |
| CDR3α | *TRAJ40* | Asp90 | Lys4 | | 1 | |
| | *TRAJ40* | Ser91 | Lys4 | | 2 | |
| | *TRAJ40* | Ala92 | | Thr163 | 1 | |
| | *TRAJ40* | Ala92 | Lys4 | | 3 | |
| | *TRAJ40* | Thr93 | | Lys66 | 2 | |
| | *TRAJ40* | Thr93 | | Trp167 | 1 | |
| | *TRAJ40* | Thr93 | Ile1 | | 2 | |
| | *n/a* | $Ala94^{O}$ | $Lys4^{N\zeta}$ | | 3 | 1 |
| | *n/a* | Leu95 | | Gly62 | 1 | |
| | *n/a* | Leu95 | Lys4 | | 2 | |
| | *n/a* | $Pro96^{O}$ | $Lys4^{N\zeta}$ | | 1 | 1 |
| | *TRAJ40* | Tyr97 | | Lys66 | 2 | |
| | *TRAJ40* | Tyr97 | | Ala69 | 1 | |
| | *TRAJ40* | Tyr97 | Lys4 | | 11 | |
| | *TRAJ40* | Tyr97 | Leu6 | | 4 | |
| CDR1β | *TRBV6* | Glu30 | Trp8 | | 8 | |
| CDR2β | *n/a* | Ile50 | Trp8 | | 5 | |
| | *n/a* | His51 | | Val76 | 3 | |
| | *n/a* | His51 | Trp8 | | 4 | |
| | *n/a* | Tyr54 | | Gln72 | 12 | |
| | *TRBV6* | $Asp56^{O\delta 2}$ | | $Arg65^{N\varepsilon}$ | 2 | 1 |
| CDR3β | *TRBJ1-1* | Tyr95 | | Lys146 | 3 | |
| | *TRBJ1-1* | Pro95 | | Ala150 | 2 | |
| | *TRBJ1-1* | Gln96 | | Lys146 | 1 | |
| | *TRBJ1-1* | Gln96 | | Trp147 | 5 | |
| | *TRBJ1-1* | Gln96 | | Ala150 | 1 | |
| | *TRBJ1-1* | Gln96 | | Val152 | 1 | |
| | *TRBJ1-1* | Gln96 | Leu6 | | 2 | |
| | *TRBJ1-1* | Gln96 | His7 | | 4 | |
| | *TRBJ1-1* | Gln96 | Trp8 | | 2 | |
| | *TRBJ1* | $Gly97^{O}$ | | $Gln155^{O\varepsilon 1}$ | | 1 |
| | *TRBJ1* | $Thr98^{O\delta 1}$ | | $Ala150^{O}$ | 5 | 1 |

* A 3.4-Å cutoff was used for H-bonds and salt bridges, and a 4-Å cutoff was used for van der Waals (vdW).

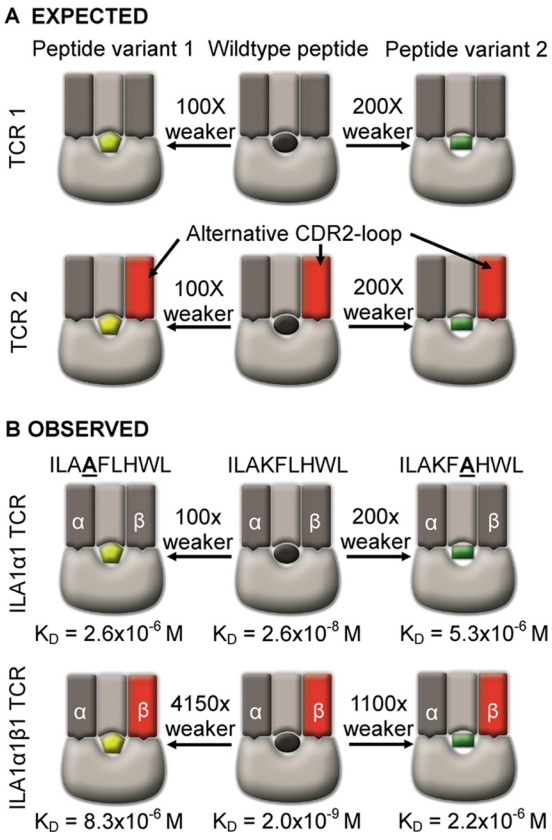


FIGURE 6. **Schematic of the effect of alanine peptide substitutions on TCR-pMHC binding affinity.** Nonmutated TCR and pMHC components are shown in grayscale. TCRs with high affinity mutations are shown in *red*. Peptide mutations are shown in *yellow* or *green*. *A,* expected difference in the binding of an unmodified TCR (TCR1) compared with a CDR2 loop mutated TCR (TCR2) (mutation shown in *red*), assuming that the CDR2 loops bind independently of the TCR-peptide interaction. Because the mutated CDR2 loop (shown in *red*) does not contact the peptide, the theoretical difference in binding between the TCR1 and TCR2 to peptide variants 1 (*yellow*) and 2 (*green*) compared with the wild-type peptide (*black*) should be identical according the interaction between the CDR3 loops and the peptide. *B,* schematic of the observed difference in the binding of the ILA1 $\alpha 1\beta 1$ TCR, compared with the ILA1 $\alpha 1$ TCR engaging a peptide-MHC complex. These data show that a disproportionate knock-on effect in binding occurs for the ILA1 $\alpha 1\beta 1$ TCR, compared with the ILA1 $\alpha 1$ TCR. These data indicate that TCR-MHC binding does not occur independently of TCR-peptide interactions and that the latter likely governs the former.

shows that the interaction between TCR and antigenic peptide can play a minimal structural role, often being responsible for less than a third of the binding interface relative to contacts between the TCR and MHC (5). Thus, the molecular mechanism by which the TCR maintains peptide-specific recognition is not immediately obvious.

To re-examine how the TCR CDR loops co-operatively act to stabilize TCR-pMHC binding, we designed a range of soluble TCRs that exhibited up to a 18,500-fold enhancement in affinity for cognate antigen using CDR loop mutations selected by phage display (26). Previous studies using high affinity TCRs have shown that these artificial reagents retain a high level of antigen specificity similar to their wild type progenitors (34, 46–48). In all cases, the enhanced affinity observed for the mutated TCRs compared with the wild type TCRs was due to small differences in the on-rate but a vastly extended off-rate. The slower off-rate indicated that any initial "transition state" was less important than the formation of a stable complex during high affinity TCR-pMHC binding. These high affinity TCRs enabled modification to the TCR-peptide interaction while retaining a strong enough residual TCR-pMHC affinity to measure using SPR. Furthermore, we were able to incorporate mutations into individual CDR loops to generate a panel of TCRs with an identical sequence except for their CDR2 loops. Structural analyses confirmed that these loops were distal to peptide binding in both wild type and enhanced affinity MEL5 and ILA1 TCRs. Based on some models of TCR engagement (11), we reasoned that HLA A*0201-restricted TCRs with high affinity mutations in their CDR2 loops should retain a residual ability to bind to the surface of HLA A*0201 independently of the peptide because the TCR-peptide interactions should only account for a small proportion of the overall binding energy. In contrast to this prediction, we were unable to show binding to the HLA A*0201-GLGGGGGGV or HLA A*0201-ALAAAAAAV null antigens with any of the CDR2 loop high affinity TCRs tested. These observations support the notion that specific interactions between the TCR and peptide are required to allow the TCR to effectively engage MHC. Using this system, we were also able to examine whether subtle alterations in the interaction between TCR and peptide were independent of TCR CDR2 loop binding to MHC. To investigate this, we tested the binding affinity of a panel of HLA A*0201-ILAKFLHWL-specific CDR2 loop-modified TCRs to peptides that contained alanine substitutions at positions structurally shown to be key TCR contacts. These data revealed that even minimal changes to the TCR-peptide interaction had a substantial impact on the TCR affinity and binding energy ($\Delta G$). These data show that TCR-peptide contacts are strongly "coupled" to TCR-MHC contacts.

We also performed a kinetic investigation of the effect of altering the TCR-peptide interaction. These data showed that the vastly extended off-rates that governed the enhanced affinity of the high affinity mutated TCRs were effectively nullified by altering the TCR interaction with peptide, although the on-rates remained relatively unchanged. Thus, our data indicate that complex formation is not initiated by TCR-MHC binding. Rather, successful TCR-peptide sampling must precede or occur at the same time as the stabilizing interaction between the TCR and the MHC surface. In support of this notion, our data show that altering the TCR interaction with peptide can override the optimal formation of TCR-MHC interactions resulting in a disproportionate knock-on effect on TCR-pMHC affinity.

Mounting evidence from other studies also contests the notion that conserved interactions between the germ line-encoded loops of the TCR and the MHC initiate TCR-pMHC complex formation. First, Burrows *et al.* (16) have demonstrated that disrupting conserved interactions between the TCR and MHC surface resulted in the formation of compensatory interactions. In support of these data, Dyson and co-workers (49) extensively diversified CDR1 and CDR2 loops *in vivo* and demonstrated that the TCR is not genetically hardwired to engage MHC ligands. Second, a number of molecular studies are incompatible with TCR-MHC initiated binding. These include the following: (i) the co-crystal structure of a TCR bound to MHCI complexed with a 13-mer "super-bulged" pep-

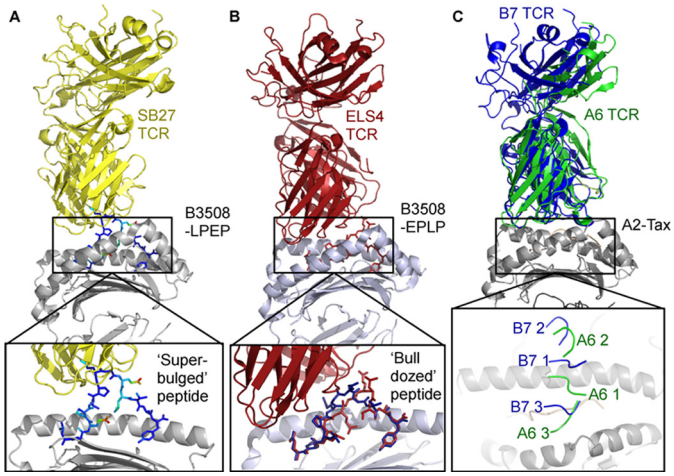


FIGURE 7. **Structural evidence demonstrating that TCR-peptide contacts precede TCR-MHC contacts.** *A,* co-crystal structure of the SB27 TCR (shown as *yellow schematic*) bound to the HLA-B*3508 (shown as *gray yellow schematic*) LPEP super-bulged 13-mer peptide (shown as *sticks*, colored using Wilson "B" factor) complex. The *expanded panel below* illustrates the extended conformation of the peptide, making it highly improbable that the SB27 TCR could contact the MHC surface before the peptide (19). *B,* co-crystal structure of the ELS4 TCR (shown as *red yellow schematic*) bound to the HLA-B*3501 (shown as *gray yellow schematic*) EPLP 11-mer peptide (shown as *sticks*, colored using *red* complexed to the ELS4 TCR and in *blue* uncomplexed). The *expanded panel below* illustrates how the EPLP peptide is bulldozed into a different conformation during TCR binding (before TCR binding is shown in *blue* and after TCR binding is shown in *red*), allowing the TCR to contact the MHC surface (20). *C,* co-crystal structure of the A6 TCR (shown as *green schematic*) superposed with the B7 TCR (shown as *blue schematic*) which both bind to the HLA A*0201 (shown as *gray schematic*) Tax (shown as *peach schematic*) complex (27, 51, 52). These TCRs share the same $\beta$-chain germ line-encoded CDR1 and CDR2 loops, and they bind to the same N-terminal region of the A2-Tax complex. The *expanded panel below* illustrates that the CDR3 loops engage some of the same residues of the peptide, whereas the CDR1 and CDR2 loops bind to distinct regions of the MHC surface.

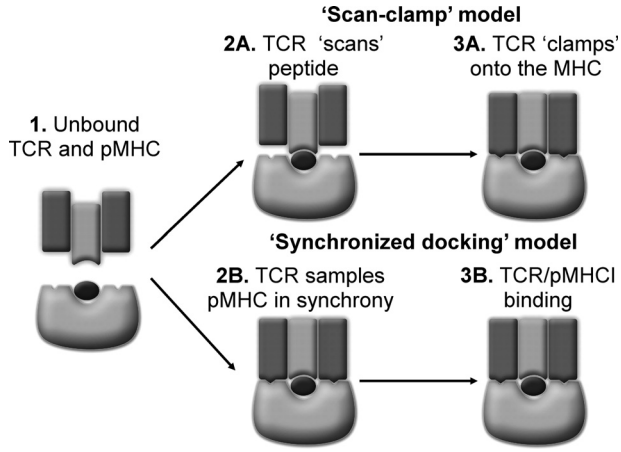


FIGURE 8. **New models for TCR engagement of pMHC.** *1.* schematic of a TCR (*dark* and *light gray*) proceeding engagement of peptide (*black*)-MHC (*light gray*). *A,* "Scan-clamp" model. Only specific TCR-peptide contacts (*light gray* and *black*) (*2A*) allow the TCR (shown in *dark gray*) to clamp-onto the MHC surface and (*3A*) complete TCR-pMHC docking, which leads to T-cell activation. *B,* "synchronized docking" model. TCR contacts the peptide and MHC simultaneously (*2B*), but TCR-peptide interactions are dominant over TCR-MHC interactions (*3B*). Only the scan clamp and synchronized docking models for T-cell antigen recognition are permissive with our data.

tide (19) showing that the extended central peptide bulge physically restricted the TCR from contacting the MHC surface (Fig. 7*A*) (19); (ii) the co-crystal structure of a TCR bound to MHCI complexed with an 11-mer peptide demonstrating that the peptide was "bulldozed" or flattened by the TCR, allowing the TCR to contact the MHC surface (Fig. 7*B*) (20); (iii) accumulated studies showing that TCR-MHC interactions can play a minimal energetic role, compared with TCR-peptide interactions, during TCR binding to MHC (15, 18, 21, 50), and (iv) the structures of the A6 and B7 TCRs bound to HLA A*0201-LLFGYPVYV (27, 51, 52), showing that, despite both TCRs sharing a genetically identical germ line-encoded V$\beta$-gene (V$\beta$6-5), the TCR-MHC contacts were distinct, although a number of identical TCR-peptide contacts existed (Fig. 7*C*). Finally, our data, in which we have tested affinity-enhanced TCRs against a range of normal tissue cell samples, show that high affinity CDR2 mutations do not render the TCRs more unspecific than high affinity CDR3 mutations. The examples above are consistent with a model for T-cell antigen recognition in which TCR-peptide binding overrides TCR-MHC engagement.

The idea that TCR-peptide contacts govern T-cell antigen recognition is in accord with several biological requirements of T-cell immunity. First, given that extremely weak TCR binding is required for positive selection of peptide-dependent T-cells in the thymus (53), control of this delicate aspect would represent a far greater challenge were TCR-MHC contacts to proceed TCR-peptide interactions (11). Second, accumulated studies that have demonstrated that alloreactive TCR recognition is peptide-dependent (54–56) are favored by models where TCR-peptide contacts dominate TCR engagement. Third, if TCR-MHC interactions initiate antigen recognition then the extraordinarily rapid kinetics of CD8 and CD4 coreceptor binding might enable aberrant T-cell signaling, bypassing antigen-specific TCR-peptide sampling (57). Fourth, a system where TCR-MHC contacts dominate TCR binding is difficult to reconcile with the kinetic segregation model of T-cell activation (58, 59). In this model, small molecules such as CD2 and CD28 facilitate contact zones to enable the TCR to scan pMHCs. The proximity of the T-cell and target cell membranes in these contact zones excludes large phosphatase molecules, such as CD45, triggering phosphorylation of the TCR and downstream signaling events. Thus, TCR-MHC binding in these contact zones could enable TCR phosphorylation independently of TCR-peptide binding. Finally, a mode of action that requires that the TCR interacts with MHC prior to peptide scanning wastes both time and energy. This is particularly important for a system that requires an individual TCR to scan a multitude of pMHC molecules to locate a cognate peptide.

We propose two new models of TCR-pMHC binding that are accommodated by our data and are both temporally and energetically complementary with a system requiring recognition of self in the thymus and rapid intolerance of non-self in the periphery. First, the "scan-clamp" model, in which the TCR "scans" the peptide before "clamping" onto the MHC surface (Fig. 8*A*). Second, the "synchronized docking" model, in which there is no temporal separation between the TCR binding to the peptide or MHC, but TCR-peptide interactions are dominant over TCR-MHC interactions (Fig. 8*B*). These new models are consistent with the requirement for T-cells to target cells based on their antigenic peptide, allowing them to expeditiously distinguish aberrant cells from healthy cells (60–63).

In conclusion, it is clear that T-cells have evolved to ensure that TCR-pMHC binding is carefully balanced to guarantee that the fidelity of antigen recognition is permissive for the conserved and universal interactions that lead to T-cell activation. Our new data shed light on the mechanisms controlling the seemingly paradoxical observation that a receptor-ligand (TCR-pMHC) interaction with both a self (TCR-MHC) and non-self (TCR-peptide) component can control T-cells by only forming productive interactions when encountering alien antigen.

*Acknowledgments—We thank Anton P. van der Merwe, Simon J. Davis, and David H. Margulies for critical reading of the manuscript and helpful discussions. We thank the staff at Diamond Light Source for providing facilities and support.*

## REFERENCES


1. Davis, M. M., and Bjorkman, P. J. (1988) T-cell antigen receptor genes and T-cell recognition. *Nature* **334,** 395–402
2. Garcia, K. C., Degano, M., Speir, J. A., and Wilson, I. A. (1999) Emerging principles for T cell receptor recognition of antigen in cellular immunity. *Rev. Immunogenet.* **1,** 75–90
3. Mason, D. (1998) A very high level of crossreactivity is an essential feature of the T-cell receptor. *Immunol. Today* **19,** 395–404
4. Sewell, A. K. (2012) Why must T cells be cross-reactive? *Nat. Rev. Immunol.* **12,** 669–677
5. Rudolph, M. G., Stanfield, R. L., and Wilson, I. A. (2006) How TCRs bind MHCs, peptides, and coreceptors. *Annu. Rev. Immunol.* **24,** 419–466
6. Gras, S., Burrows, S. R., Turner, S. J., Sewell, A. K., McCluskey, J., and Rossjohn, J. (2012) A structural voyage toward an understanding of the MHC-I-restricted immune response: lessons learned and much to be learned. *Immunol. Rev.* **250,** 61–81
7. Dai, S., Huseby, E. S., Rubtsova, K., Scott-Browne, J., Crawford, F., Macdonald, W. A., Marrack, P., and Kappler, J. W. (2008) Crossreactive T cells spotlight the germ line rules for $\alpha\beta$ T cell-receptor interactions with MHC molecules. *Immunity* **28,** 324–334
8. Feng, D., Bond, C. J., Ely, L. K., Maynard, J., and Garcia, K. C. (2007) Structural evidence for a germ line-encoded T cell receptor-major histocompatibility complex interaction "codon." *Nat. Immunol.* **8,** 975–983
9. Garcia, K. C., Adams, J. J., Feng, D., and Ely, L. K. (2009) The molecular basis of TCR germ line bias for MHC is surprisingly simple. *Nat. Immunol.* **10,** 143–147
10. Scott-Browne, J. P., White, J., Kappler, J. W., Gapin, L., and Marrack, P. (2009) Germ line-encoded amino acids in the $\alpha\beta$ T-cell receptor control thymic selection. *Nature* **458,** 1043–1046
11. Wu, L. C., Tuot, D. S., Lyons, D. S., Garcia, K. C., and Davis, M. M. (2002) Two-step binding mechanism for T-cell receptor recognition of peptide MHC. *Nature* **418,** 552–556
12. Housset, D., and Malissen, B. (2003) What do TCR-pMHC crystal structures teach us about MHC restriction and alloreactivity? *Trends Immunol.* **24,** 429–437
13. Wooldridge, L., Ekeruche-Makinde, J., van den Berg, H. A., Skowera, A., Miles, J. J., Tan, M. P., Dolton, G., Clement, M., Llewellyn-Lacey, S., Price, D. A., Peakman, M., and Sewell, A. K. (2012) A single autoimmune T cell receptor recognizes more than a million different peptides. *J. Biol. Chem.* **287,** 1168–1177
14. Colf, L. A., Bankovich, A. J., Hanick, N. A., Bowerman, N. A., Jones, L. L., Kranz, D. M., and Garcia, K. C. (2007) How a single T cell receptor recognizes both self and foreign MHC. *Cell* **129,** 135–146
15. Borg, N. A., Ely, L. K., Beddoe, T., Macdonald, W. A., Reid, H. H., Clements, C. S., Purcell, A. W., Kjer-Nielsen, L., Miles, J. J., Burrows, S. R., McCluskey, J., and Rossjohn, J. (2005) The CDR3 regions of an immunodominant T cell receptor dictate the "energetic landscape" of peptide-MHC recognition. *Nat. Immunol.* **6,** 171–180
16. Burrows, S. R., Chen, Z., Archbold, J. K., Tynan, F. E., Beddoe, T., Kjer-Nielsen, L., Miles, J. J., Khanna, R., Moss, D. J., Liu, Y. C., Gras, S., Kostenko, L., Brennan, R. M., Clements, C. S., Brooks, A. G., Purcell, A. W., McCluskey, J., and Rossjohn, J. (2010) Hard wiring of T cell receptor specificity for the major histocompatibility complex is underpinned by TCR adaptability. *Proc. Natl. Acad. Sci. U.S.A.* **107,** 10608–10613
17. Gras, S., Chen, Z., Miles, J. J., Liu, Y. C., Bell, M. J., Sullivan, L. C., Kjer-Nielsen, L., Brennan, R. M., Burrows, J. M., Neller, M. A., Khanna, R., Purcell, A. W., Brooks, A. G., McCluskey, J., Rossjohn, J., and Burrows, S. R. (2010) Allelic polymorphism in the T cell receptor and its impact on immune responses. *J. Exp. Med.* **207,** 1555–1567
18. Sethi, D. K., Schubert, D. A., Anders, A. K., Heroux, A., Bonsor, D. A., Thomas, C. P., Sundberg, E. J., Pyrdol, J., and Wucherpfennig, K. W. (2011) A highly tilted binding mode by a self-reactive T cell receptor results in altered engagement of peptide and MHC. *J. Exp. Med.* **208,** 91–102
19. Tynan, F. E., Burrows, S. R., Buckle, A. M., Clements, C. S., Borg, N. A., Miles, J. J., Beddoe, T., Whisstock, J. C., Wilce, M. C., Silins, S. L., Burrows, J. M., Kjer-Nielsen, L., Kostenko, L., Purcell, A. W., McCluskey, J., and Rossjohn, J. (2005) T cell receptor recognition of a "super-bulged" major histocompatibility complex class I-bound peptide. *Nat. Immunol.* **6,** 1114–1122
20. Tynan, F. E., Reid, H. H., Kjer-Nielsen, L., Miles, J. J., Wilce, M. C., Kostenko, L., Borg, N. A., Williamson, N. A., Beddoe, T., Purcell, A. W., Burrows, S. R., McCluskey, J., and Rossjohn, J. (2007) A T cell receptor flattens a bulged antigenic peptide presented by a major histocompatibility complex class I molecule. *Nat. Immunol.* **8,** 268–276
21. Yin, Y., Li, Y., Kerzic, M. C., Martin, R., and Mariuzza, R. A. (2011) Structure of a TCR with high affinity for self-antigen reveals basis for escape from negative selection. *EMBO J.* **30,** 1137–1148
22. Bridgeman, J. S., Sewell, A. K., Miles, J. J., Price, D. A., and Cole, D. K. (2012) Structural and biophysical determinants of $\alpha\beta$ T-cell antigen recognition. *Immunology* **135,** 9–18
23. Cole, D. K., Pumphrey, N. J., Boulter, J. M., Sami, M., Bell, J. I., Gostick, E., Price, D. A., Gao, G. F., Sewell, A. K., and Jakobsen, B. K. (2007) Human TCR-binding affinity is governed by MHC class restriction. *J. Immunol.* **178,** 5727–5734
24. Cole, D. K., Yuan, F., Rizkallah, P. J., Miles, J. J., Gostick, E., Price, D. A., Gao, G. F., Jakobsen, B. K., and Sewell, A. K. (2009) Germ line-governed recognition of a cancer epitope by an immunodominant human T-cell receptor. *J. Biol. Chem.* **284,** 27281–27289
25. Purbhoo, M. A., Li, Y., Sutton, D. H., Brewer, J. E., Gostick, E., Bossi, G., Laugel, B., Moysey, R., Baston, E., Liddy, N., Cameron, B., Bennett, A. D., Ashfield, R., Milicic, A., Price, D. A., Classon, B. J., Sewell, A. K., and Jakobsen, B. K. (2007) The HLA A*0201-restricted hTERT(540–548) peptide is not detected on tumor cells by a CTL clone or a high-affinity T-cell receptor. *Mol. Cancer Ther.* **6,** 2081–2091
26. Li, Y., Moysey, R., Molloy, P. E., Vuidepot, A. L., Mahon, T., Baston, E., Dunn, S., Liddy, N., Jacob, J., Jakobsen, B. K., and Boulter, J. M. (2005) Directed evolution of human T-cell receptors with picomolar affinities by phage display. *Nat. Biotechnol.* **23,** 349–354
27. Garboczi, D. N., Ghosh, P., Utz, U., Fan, Q. R., Biddison, W. E., and Wiley, D. C. (1996) Structure of the complex between human T-cell receptor, viral peptide and HLA-A2. *Nature* **384,** 134–141
28. Boulter, J. M., Glick, M., Todorov, P. T., Baston, E., Sami, M., Rizkallah, P., and Jakobsen, B. K. (2003) Stable, soluble T-cell receptor molecules for crystallization and therapeutics. *Protein Eng.* **16,** 707–711
29. Cole, D. K., Dunn, S. M., Sami, M., Boulter, J. M., Jakobsen, B. K., and Sewell, A. K. (2008) T cell receptor engagement of peptide-major histocompatibility complex class I does not modify CD8 binding. *Mol. Immunol.* **45,** 2700–2709
30. Cole, D. K., Rizkallah, P. J., Gao, F., Watson, N. I., Boulter, J. M., Bell, J. I., Sami, M., Gao, G. F., and Jakobsen, B. K. (2006) Crystal structure of HLA-A*2402 complexed with a telomerase peptide. *Eur. J. Immunol.* **36,** 170–179
31. Wyer, J. R., Willcox, B. E., Gao, G. F., Gerth, U. C., Davis, S. J., Bell, J. I., van der Merwe, P. A., and Jakobsen, B. K. (1999) T cell receptor and coreceptor CD8 $\alpha\alpha$ bind peptide-MHC independently and with distinct kinetics. *Immunity* **10,** 219–225

32. Holland, C. J., Rizkallah, P. J., Vollers, S., Calvo-Calle, J. M., Madura, F., Fuller, A., Sewell, A. K., Stern, L. J., Godkin, A., and Cole, D. K. (2012) Minimal conformational plasticity enables TCR cross-reactivity to different MHC class II heterodimers. *Sci. Rep.* **2,** 629
33. Miles, J. J., Bulek, A. M., Cole, D. K., Gostick, E., Schauenburg, A. J., Dolton, G., Venturi, V., Davenport, M. P., Tan, M. P., Burrows, S. R., Wooldridge, L., Price, D. A., Rizkallah, P. J., and Sewell, A. K. (2010) Genetic and structural basis for selection of a ubiquitous T cell receptor deployed in Epstein-Barr virus infection. *PLoS Pathog.* **6,** e1001198
34. Madura, F., Rizkallah, P. J., Miles, K. M., Holland, C. J., Bulek, A. M., Fuller, A., Schauenburg, A. J., Miles, J. J., Liddy, N., Sami, M., Li, Y., Hossain, M., Baker, B. M., Jakobsen, B. K., Sewell, A. K., and Cole, D. K. (2013) T-cell receptor specificity maintained by altered thermodynamics. *J. Biol. Chem.* **288,** 18766–18775
35. Karlsson, R., Katsamba, P. S., Nordin, H., Pol, E., and Myszka, D. G. (2006) Analyzing a kinetic titration series using affinity biosensors. *Anal. Biochem.* **349,** 136–147
36. Winter, G. (2010) xia2: an expert system for macromolecular crystallography data reduction. *J. Appl. Crystallogr.* **43,** 186–190
37. Collaborative Computational Project No. 4 (1994) The CCP4 suite: programs for protein crystallography. *Acta Crystallogr. D Biol. Crystallogr.* **50,** 760–763
38. McCoy, A. J., Grosse-Kunstleve, R. W., Adams, P. D., Winn, M. D., Storoni, L. C., and Read, R. J. (2007) Phaser crystallographic software. *J. Appl. Crystallogr.* **40,** 658–674
39. Emsley, P., and Cowtan, K. (2004) Coot: model-building tools for molecular graphics. *Acta Crystallogr. D Biol. Crystallogr.* **60,** 2126–2132
40. Delano, W. L. (2002) *The PyMOL Molecular Graphics System*, DeLano Scientific LLC, San Carlos, CA
41. Cole, D. K., Sami, M., Scott, D. R., Rizkallah, P. J., Borbulevych, O. Y., Todorov, P. T., Moysey, R. K., Jakobsen, B. K., Boulter, J. M., Baker, B. M., and Yi, L. (2013) Increased peptide contacts govern high affinity binding of a modified TCR whilst maintaining a native pMHC docking mode. *Front. Immunol.* **4,** 168
42. Dunn, S. M., Rizkallah, P. J., Baston, E., Mahon, T., Cameron, B., Moysey, R., Gao, F., Sami, M., Boulter, J., Li, Y., and Jakobsen, B. K. (2006) Directed evolution of human T cell receptor CDR2 residues by phage display dramatically enhances affinity for cognate peptide-MHC without increasing apparent cross-reactivity. *Protein Sci.* **15,** 710–721
43. Sami, M., Rizkallah, P. J., Dunn, S., Molloy, P., Moysey, R., Vuidepot, A., Baston, E., Todorov, P., Li, Y., Gao, F., Boulter, J. M., and Jakobsen, B. K. (2007) Crystal structures of high affinity human T-cell receptors bound to peptide major histocompatibility complex reveal native diagonal binding geometry. *Protein Eng. Des. Sel.* **20,** 397–403
44. Varela-Rohena, A., Molloy, P. E., Dunn, S. M., Li, Y., Suhoski, M. M., Carroll, R. G., Milicic, A., Mahon, T., Sutton, D. H., Laugel, B., Moysey, R., Cameron, B. J., Vuidepot, A., Purbhoo, M. A., Cole, D. K., Phillips, R. E., June, C. H., Jakobsen, B. K., Sewell, A. K., and Riley, J. L. (2008) Control of HIV-1 immune escape by CD8 T cells expressing enhanced T-cell receptor. *Nat. Med.* **14,** 1390–1395
45. Tickle, I. J., Laskowski, R. A., and Moss, D. S. (2000) Rfree and the Rfree ratio. II. Calculation of the expected values and variances of cross-validation statistics in macromolecular least-squares refinement. *Acta Crystallogr. D Biol. Crystallogr.* **56,** 442–450
46. Donermeyer, D. L., Weber, K. S., Kranz, D. M., and Allen, P. M. (2006) The study of high-affinity TCRs reveals duality in T cell recognition of antigen: specificity and degeneracy. *J. Immunol.* **177,** 6911–6919
47. Laugel, B., Boulter, J. M., Lissin, N., Vuidepot, A., Li, Y., Gostick, E., Crotty, L. E., Douek, D. C., Hemelaar, J., Price, D. A., Jakobsen, B. K., and Sewell, A. K. (2005) Design of soluble recombinant T cell receptors for antigen targeting and T cell inhibition. *J. Biol. Chem.* **280,** 1882–1892
48. Persaud, S. P., Donermeyer, D. L., Weber, K. S., Kranz, D. M., and Allen, P. M. (2010) High-affinity T cell receptor differentiates cognate peptide-MHC and altered peptide ligands with distinct kinetics and thermodynamics. *Mol. Immunol.* **47,** 1793–1801
49. Holland, S. J., Bartok, I., Attaf, M., Genolet, R., Luescher, I. F., Kotsiou, E., Richard, A., Wang, E., White, M., Coe, D. J., Chai, J. G., Ferreira, C., and Dyson, J. (2012) The T-cell receptor is not hardwired to engage MHC ligands. *Proc. Natl. Acad. Sci. U.S.A.* **109,** E3111–3118
50. Piepenbrink, K. H., Blevins, S. J., Scott, D. R., and Baker, B. M. (2013) The basis for limited specificity and MHC restriction in a T cell receptor interface. *Nat. Commun.* **4,** 1948
51. Ding, Y. H., Baker, B. M., Garboczi, D. N., Biddison, W. E., and Wiley, D. C. (1999) Four A6-TCR/peptide/HLA-A2 structures that generate very different T cell signals are nearly identical. *Immunity* **11,** 45–56
52. Ding, Y. H., Smith, K. J., Garboczi, D. N., Utz, U., Biddison, W. E., and Wiley, D. C. (1998) Two human T cell receptors bind in a similar diagonal mode to the HLA-A2/Tax peptide complex using different TCR amino acids. *Immunity* **8,** 403–411
53. Alam, S. M., Travers, P. J., Wung, J. L., Nasholds, W., Redpath, S., Jameson, S. C., and Gascoigne, N. R. (1996) T-cell-receptor affinity and thymocyte positive selection. *Nature* **381,** 616–620
54. Archbold, J. K., Macdonald, W. A., Miles, J. J., Brennan, R. M., Kjer-Nielsen, L., McCluskey, J., Burrows, S. R., and Rossjohn, J. (2006) Alloreactivity between disparate cognate and allogeneic pMHC-I complexes is the result of highly focused, peptide-dependent structural mimicry. *J. Biol. Chem.* **281,** 34324–34332
55. Macdonald, W. A., Chen, Z., Gras, S., Archbold, J. K., Tynan, F. E., Clements, C. S., Bharadwaj, M., Kjer-Nielsen, L., Saunders, P. M., Wilce, M. C., Crawford, F., Stadinsky, B., Jackson, D., Brooks, A. G., Purcell, A. W., Kappler, J. W., Burrows, S. R., Rossjohn, J., and McCluskey, J. (2009) T cell allorecognition via molecular mimicry. *Immunity* **31,** 897–908
56. Reiser, J. B., Darnault, C., Guimezanes, A., Grégoire, C., Mosser, T., Schmitt-Verhulst, A. M., Fontecilla-Camps, J. C., Malissen, B., Housset, D., and Mazza, G. (2000) Crystal structure of a T cell receptor bound to an allogeneic MHC molecule. *Nat. Immunol.* **1,** 291–297
57. van der Merwe, P. A., and Davis, S. J. (2003) Molecular interactions mediating T cell antigen recognition. *Annu. Rev. Immunol.* **21,** 659–684
58. Choudhuri, K., Wiseman, D., Brown, M. H., Gould, K., and van der Merwe, P. A. (2005) T-cell receptor triggering is critically dependent on the dimensions of its peptide-MHC ligand. *Nature* **436,** 578–582
59. Davis, S. J., and van der Merwe, P. A. (2006) The kinetic-segregation model: TCR triggering and beyond. *Nat. Immunol.* **7,** 803–809
60. Dustin, M. L., Bromley, S. K., Kan, Z., Peterson, D. A., and Unanue, E. R. (1997) Antigen receptor engagement delivers a stop signal to migrating T lymphocytes. *Proc. Natl. Acad. Sci. U.S.A.* **94,** 3909–3913
61. Mempel, T. R., Henrickson, S. E., and Von Andrian, U. H. (2004) T-cell priming by dendritic cells in lymph nodes occurs in three distinct phases. *Nature* **427,** 154–159
62. Negulescu, P. A., Krasieva, T. B., Khan, A., Kerschbaum, H. H., and Cahalan, M. D. (1996) Polarity of T cell shape, motility, and sensitivity to antigen. *Immunity* **4,** 421–430
63. Schneider, H., Downey, J., Smith, A., Zinselmeyer, B. H., Rush, C., Brewer, J. M., Wei, B., Hogg, N., Garside, P., and Rudd, C. E. (2006) Reversal of the TCR stop signal by CTLA-4. *Science* **313,** 1972–1975
64. Chen, J. L., Stewart-Jones, G., Bossi, G., Lissin, N. M., Wooldridge, L., Choi, E. M., Held, G., Dunbar, P. R., Esnouf, R. M., Sami, M., Boulter, J. M., Rizkallah, P., Renner, C., Sewell, A., van der Merwe, P. A., Jakobsen, B. K., Griffiths, G., Jones, E. Y., and Cerundolo, V. (2005) Structural and kinetic basis for heightened immunogenicity of T cell vaccines. *J. Exp. Med.* **201,** 1243–1255